Expandable Graphite-Methyl Methacrylate-Acrylic Acid Copolymer Composite Particles as a Flame Retardant of Rigid Polyurethane Foam

Xiao-Guang Zhang,[1] Lan-Lan Ge,[1] Wei-Qin Zhang,[2] Jian-Hua Tang,[1] Ling Ye,[2] Zhong-Ming Li[2]

[1]*College of Chemical Engineering, Sichuan University, Chengdu 610065, People's Republic of China*
[2]*College of Polymer Science and Engineering, State Key Laboratory of Polymer Materials Engineering, Sichuan University, Chengdu 610065, People's Republic of China*

Received 11 November 2010; accepted 20 January 2011
DOI 10.1002/app.34198
Published online 19 May 2011 in Wiley Online Library (wileyonlinelibrary.com).

ABSTRACT: An emulsion polymerization method was employed to prepare pulverized expandable graphite (pEG)-poly(methyl methacrylate-acrylic acid) copolymer [(PMA)] composite particles, and then the pEG-P(MA) particles were used for a flame retardant of the rigid polyurethane foam (RPUF). Fourier transform infrared (FTIR) spectroscopy data demonstrated the existence of P(MA) in the pEG-P(MA) particles, and the result of the thermogravimetric analysis (TGA) indicated that the content of P(MA) was 24.3 wt %. Morphological observation showed that the pEG particles were encapsulated by a layer of polymer coating to form typical core–shell composite particles. Due to the possible reaction between —COOH of pEG-P(MA) and *R*-CNO of isocyanate, the compatibility between the composite particles and the RPUF matrix was highly enhanced. In contrast to the pEG, the limiting oxygen index (LOI), the horizontal and vertical burning tests showed the pEG-P(MA) composite particles could improve the flame retardancy effectively. The improved flame retardancy of the RPUF matrix was attributed to the increased expansion volume ratio of pEG-P(MA) particles as exposed to fire. The dynamical mechanical analysis (DMA) showed that the incorporation of the core–shell particles could improve the storage modulus and tan δ of the RPUF composites. © 2011 Wiley Periodicals, Inc. J Appl Polym Sci 122: 932–941, 2011

Key words: core–shell composite particle; flame retardant; expandable graphite; rigid polyurethane foam

INTRODUCTION

Polyurethane foam (PUF) is a polymer material which is widely used in various industries such as petroleum, chemical plant and building. However, PUF is flammable and the smoke of CO, HCN, and other toxic gases releases during its burning which is very harmful to the human health and the environment.[1] Therefore, seeking desirable flame retardants for PUF is quite necessary. Because it is difficult to overcome the shortcomings of traditional halogen flame retardants, such as releasing corrosive and toxic smoke, halogen-free flame retardants are naturally attracted more and more attention, especially the intumescent flame retardants.[2] Expandable graphite (EG) is one of the halogen-free intumescent flame retardants, which has a special graphite flake structure where sulfuric acid (H_2SO_4) is intercalated between the carbon layers. When EG is exposed to fire, on one hand, the chemical reaction occurs in the case of H_2SO_4:

$$C + 2H_2SO_4 = CO_2 \uparrow + 2H_2O \uparrow + 2SO_2 \uparrow$$

On the other hand, the sulfuric acid between the carbon layers boils and decomposes into some gas.[3] Hence, when the composite material with EG is heated, EG can expand to form "worm-like" carbon layer on the surface, thus the layer limits the heat and oxygen transfer, also suppresses the release of the smokes.[4] Ultimately, the carbon coating prevents the composite material from burning.

In our previous work, we studied the influence of various factors (the loading of EG, the density of PUF, and the size of EG particles) on the flame retardant and mechanical properties of the EG-filled rigid PUF (RPUF).[5–9] It has been verified that EG could effectively improve the fire retardant performance of RPUF. However, the large-size EG particles would cause the poor adhesion between EG and RPUF matrix, thus producing the defects in the foam, e.g., collapse of cells. The mechanical

Correspondence to: J.-H. Tang (jianhuatang@ckfc.asia); Z.-M. Li (zmli@scu.edu.cn).

Contract grant sponsor: National Natural Science Foundation of China for the financial support for this subject; contract grant number: 21076128.

properties of the EG/RPUF composites were sharply deteriorated. Therefore, we pulverized the EG particles into fine ones (pEG) using an ultra-high speed mixer to reduce the destructive effects of EG on the mechanical properties of RPUF composites.[10] However, when the pEG particles were heated, the blowing gases escaped from the edge of the flakes more quickly than the raw EG particles, leading to a smaller swelling volume of the pEG particles. Their flame retardant performance was degraded.

Based on the previous work, we proposed to encapsulate the pEG particles with a thin layer of polymer coating to form core–shell flame retardant particles. When the core–shell flame retardant particles were heated, the polymer coating could prevent the blowing gases (CO_2, H_2O, and SO_2, etc.) from escaping from the edge of the flakes immediately. The swelling volume of the core–shell particles was bound to be increased, resulting in their flame retardant properties improved. Following this strategy, we have done some preliminary researches on the synthesis of pEG-poly(methyl methacrylate) (PMMA) composite particles and their application to flame retardant of RPUF.[11] The results showed that the limiting oxygen index (LOI) value of the RPUF composite containing 10 wt % of pEG-PMMA core–shell particles was increased from 23.5 vol % of pEG/RPUF composite to 26.5 vol %. When PMMA was partially hydrolyzed, the *R*-COOH group in the polymer coating would react with the *R*-NCO group of the isocyanate. Therefore, the interface adhesion between pEG-PMMA and RPUF could be highly enhanced and the mechanical properties of the RPUF composites were significantly improved.[12] Unfortunately, PMMA began to degrade at the temperature of 180°C, while the expansion temperature of the raw EG was above 200°C.[13] Hence PMMA did not effectively prevent the gas from escaping at a higher temperature and within a certain time range, which was not favorable to further improvement of the flame retardancy of the foam composite.

The aim of this work is to employ another polymer which owns a higher initial decomposition temperature as the shell material to form the core–shell flame retardant particles. When the retardant particles are heated, the pEG particles can expand to a higher expansion ratio, and further improve the flame retardant. Following such an idea, the pEG particles encapsulated with poly(methyl methacrylate-acrylic acid) copolymer [(PMA)] was prepared via emulsion polymerization.[14,15] Not only did the initial decomposition temperature of copolymer improve but also the —COOH group in the copolymer itself reacted with the *R*-NCO of isocyanate. Hence, the pEG-P(MA) shell–core composite particles filled RPUF exhibited the outstanding flame retardancy and the compatibility between pEG and matrix was enhanced.

EXPERIMENTAL

Materials

Isocyanate, Model N200, was purchased from Changfeng Chemical Co. (Chongqing, China). The primary material properties of N200 are as follows, isocyanate equivalent weight, 126.5 g, —NCO weight percent, 30%, viscosity (25°C), 215 $\times$ 10^{-3} pa.s, functionality, 2.2. Polyether polyol (PAPI), Model GR-4110G, based on the polypropylene oxide, and sucrose/glycerin base, was purchased from Gaoqiao Petro Co. (Shanghai, China). The main properties are as follows, density (25°C), 1.1 g/cm^3, hydroxyl number, 430 mg potassium hydroxide (KOH) equiv/g of resin, viscosity (25°C), 3.283 pa.s, functionality, 4.1, average molecular weight, 550 g/mol.

Triethanolamine, a cross-link catalyst with a density (25°C) of 1.122 g/cm^3, was purchased from Shanghai Chemical Reagent Co.(Shanghai, China).

Dibutyl tin dilaurate, a catalyst with a density of 1.052g/cm^3 and Sn content of 18 wt % was obtained from Sichuan Chemical Reagent Co.(Chengdu, China). Methyl methacrylate (MMA), potassium persulfate (KPS), sodium dodecyl sulfate (SDS), Sodium chloride (NaCl), dicarbonate ($NaHCO_3$), and acrylic acid (AA) were purchased from Kelong Chemical Co. (Chengdu, China). All the reagents are of analytical grade.

Synthesis of pEG-P(MA)

A 500mL four-necked round-bottom flask was equipped with a stirrer, a condenser, a thermometer and a N_2 inlet. The flask was charged with SDS (1.7 g), $NaHCO_3$ (1.3 g), H_2O (200 mL), and pEG (80 g). The flask was heated to 45°C and kept stirring for 1 h. To promote pEG dispersion, a ultrasonication treatment was also used in the above procedures. The mixture was then heated to 65°C under N_2 atmosphere for 5 min. Then KPS (15 g of 0.5 wt %) aqueous solution, MMA (10 mL) and AA (5 mL) were poured into the flask. Thereafter, the mixture was kept for about 30 min. Additional KPS (15 g of 0.5 wt %), MMA (10 mL), and AA (5 mL) were dripped into the flask within 1 h. The mixture was further kept under reflux for 4 h at 65°C. The above reaction procedures were all under N_2 atmosphere. At last, the precipitate was filtered and washed with plenteous deionized water three times after breaking emulsion by a certain concentration of sodium chloride solution. Finally, the precipitate was dried at 60°C for 4 h, yielding a deep gray powder.

Synthesis of RPUF composites

The detailed preparation procedures of RPUF were reported in our previous publications.[5–9] The

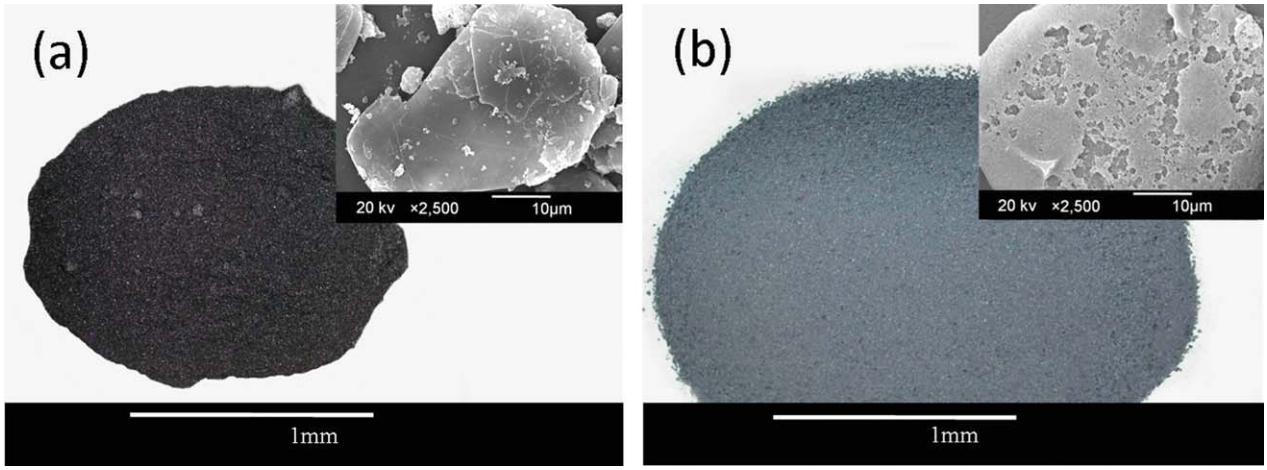

Figure 1 SEM micrographs of (a) raw pEG and (b) pEG-P(MA) [Color figure can be viewed in the online issue, which is available at wileyonlinelibrary.com].

pEG-P(MA)/RPUF and P(MA)/RPUF composites were prepared using the same way by cast molding. In this work, the pEG content was fixed at 10 wt %. The density of all the samples for further characterizations was 0.2 g/cm^3 ± 0.01 g/cm^3.

Characterizations

Fourier transform infrared (FTIR) spectroscopy was used to detect the presence of P(MA) in the core–shell particles with a Nicolet 560 FTIR spectrometer. 100 scans within the range of 4000 cm^{-1}–400 cm^{-1} were done for each sample.

Thermogravimetric analysis (TGA) was performed using a Q5000 WRT-2P instrument thermogravimetric analyzer (made in Shanghai, China) at a heating rate of 10°C/min from 50 to 800°C under N_2 atmosphere.

Fire behavior was characterized through LOI, horizontal and vertical burning tests. LOI was determined on a HC-2 oxygen index tester (Jiangning, China) according to ASTM D 2863-97. The geometry of the sample sheets was 127 × 10 × 10 mm^3 The horizontal and the vertical burning tests were conducted with a CTF-2 horizontal and vertical burning instrument (made in Jiangning, China) according to ASTM D 635-98 and ASTM 3801-96, respectively. The geometry of the sample sheets was 127 × 13 × 10 mm^3.

The morphological study was performed by a scanning electron microscope (SEM) using JSM-9600 (JEOL, Japan) with an accelerating voltage of 20 kV.

The compressive strength and the compressive modulus were measured with a universal electronic tensile machine (Shimadzu, Japan) with a compression rate of 2 mm/min according to ASTM D1621-94.

The dynamical mechanical analysis (DMA) was done by a Q800 DMA instrument (TA Instruments, USA) with a heating rate of 3°C/min. The sample size was 35 × 10 × 4mm^3. The temperature range tested was from 50 to 250°C.

RESULTS AND DISCUSSION

Morphological observation of core–shell composite particles

Figure 1 displays SEM micrographs of the raw pEG and the pEG-P(MA) particles. From Figure 1(a), one can easily see that the raw pEG presents a smooth surface due to the raw graphite flakes. Very small graphite sheets can be also found out on the surface, which were exfoliated from the raw EG particles upon the intense shear of the ultra-high speed mixer. Comparing the two micrographs in Figure 1, it is interesting to find that the surface of the pEG-P(MA) particles [Fig. 1(b)] becomes rough, the size of the particles becomes larger and no metallic luster appears. But there are so much imperfections of the coating polymer on the pEG-P(MA) particle which are mainly attributed to the fact that water molecules and monomer molecules are wrapped in the polymer during encapsulation. These small molecules are evaporated from the composite particles when dried, leaving some flaws. Above all it suggests that the pEG particles are encapsulated by a layer of polymer coating. The Scheme 1 shows the formation model of the core–shell structure of pEG-P(MA) particles and the detailed chemical reaction of polymerization of P(MA).

The pEG particles are emulsified owing to the existence of the emulsifier. And the aggregation of the copolymer of the monomer MMA and AA occurs inside micelles on the surface of the pEG particles due to the effect of the initiator.[16] When a certain chain length of the copolymer is reached, some oligomers are also formed owing to external

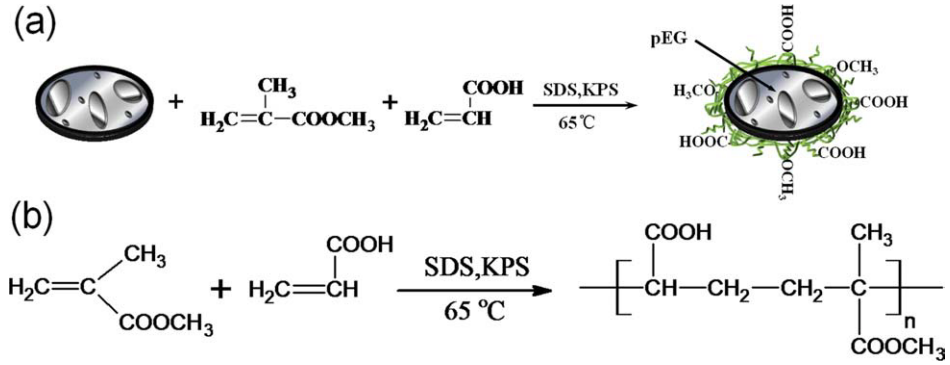

Scheme 1 Core–shell formation model of pEG-P(MA) particles (a) and chemical reaction scheme of polymerization of P(MA) (b) [Color figure can be viewed in the online issue, which is available at wileyonlinelibrary.com].

environment (such as the initiator, monomer concentration, etc.) during copolymer aggregating in micelles. At last, a large amount of the long copolymer chains form a polymer coating on the pEG surface. Unfortunately, all of the chains cannot fully grow into high degree of polymerization of copolymer chains. The copolymer would form a "strawberry-like" coating structure on the surface of the pEG particles.[17] The copolymer, including the "strawberry-like" structure coating and the coating of the long chains forms the core–shell coating on the pEG surface. The schematic illustration of this special structure is shown in Scheme 2. As is shown in Scheme 2, the —COOH group of pEG-P(MA) can react with the *R*-CNO of isocyanate. Therefore, the enhanced adhesion between the pEG-P(MA) particle and the matrix can be expected.

FTIR spectra characterization

Figure 2 shows the FTIR spectra of P(MA), pEG, and pEG-P(MA). The IR characteristic absorptions of P(MA) can be observed at 2950 cm^{-1} corresponding to symmetrical and asymmetrical absorptions of the C—H groups. The absorptions at 1450 cm^{-1} and 1390 cm^{-1} are attributed to the vibration mode of —CH_2 and —CH_3 groups, respectively. The absorption at 3430 cm^{-1} are assigned to the —OH of the —COOH groups. And, the absorptions at 1150 cm^{-1}–1250 cm^{-1} and 1731 cm^{-1} are for the stretching vibration of the —C—O group and stretching vibration of the –C=O groups, respectively. The above results confirm the existence of P(MA).

Comparing the FTIR curves of P(MA) and pEG-P(MA), one can find that both materials display the same characteristic peaks, indicating their consistent chemical groups. At the same time, the characteristic peaks of P(MA) and pEG-P(MA) do not appear in the spectra of the pEG. Combining FTIR with SEM results, a conclusion can be drawn that the pEG particles are successfully encapsulated by a polymer coating of P(MA).

Thermal analysis

The TG curves of pEG, pEG-P(MA), and P(MA) are shown in Figure 3. It can be clearly observed that the pEG particles begin to decompose at 200°C and the residual rate is 74.1 wt % at 800°C. 25.9 wt % of weight loss may be due to a redox process between H_2SO_4 and graphite, releasing the blowing gases.

The decomposition of P(MA) starts at 404°C. The mass loss rate increases with temperature, the maximum of which is 76.6 wt % in the temperature range from 404 to 452°C. And compared with PMMA, the initial decomposition temperature of P(MA) significantly increases,[11] so it is possible to improve flame retardancy of the pEG-P(MA) particles filled RPUF composites. The increased thermal stabilities of P(MA) could be due to the acid catalyst of AA

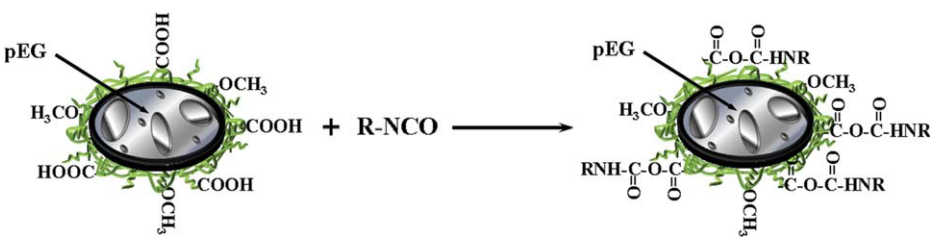

Scheme 2 Reaction scheme between the —COOH group of pEG-P(MA) and *R*-NCO of isocyanate [Color figure can be viewed in the online issue, which is available at wileyonlinelibrary.com].

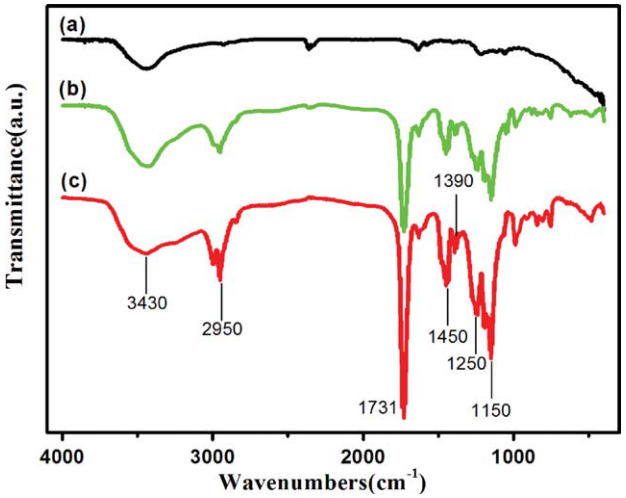

Figure 2 FTIR spectra of raw (a) pEG, (b) pEG-P(MA), and (c) P(MA) [Color figure can be viewed in the online issue, which is available at wileyonlinelibrary.com].

during the thermal degradation of copolymer, causing decomposition temperature shift to higher temperature.[18] Some reports had also proposed that monomer sequences such as methacrylic acid or acrylic acid can increase thermal stabilities of copolymers.[19–21] The residual rate of P(MA) is 2.1% when the temperature reaches 800°C. The degradation of the pEG-P(MA) exhibits two steps of decomposition. The first weight loss step from 240 to 368°C comes from the gas release during expansion of pEG in the surface of samples, in this step, pEG started to expand to form a carbon layer and shows a maximal rate of weight loss at 304°C; the second range from 368 to 416°C was due to the degradation of carbon bone mainchain of P(MA),[22–23] in this step, the expanded pEG also started to degrade and presents a maximal rate of weight loss at 398°C. The

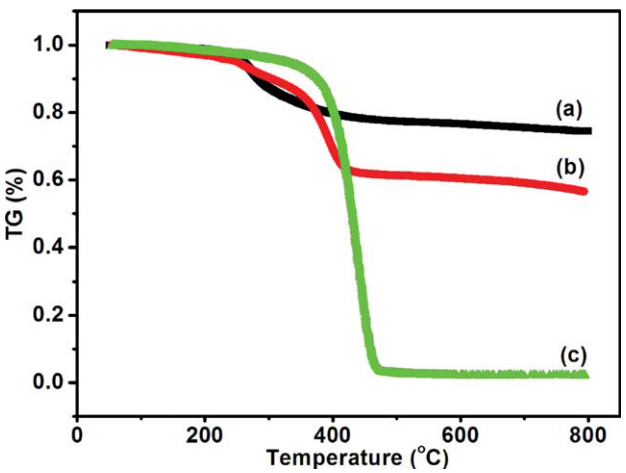

Figure 3 TG curves under N2 atm for (a) pEG, (b) pEG-P(MA), and (c) P(MA) [Color figure can be viewed in the online issue, which is available at wileyonlinelibrary.com].

residual rate of the pEG-P(MA) is 56.6 wt % at 800°C. However, we find that the beginning decomposition temperature of the pEG-P(MA) is lower than that of the pure P(MA). The reason is that the beginning expansion temperature of pEG is at about 240°C while the decomposition of P(MA) starts at 404°C. So the beginning decomposition temperature of pEG-P(MA) is lower than that of the pure P(MA) come from the gas release during expansion of pEG. Furthermore, It can be mainly ascribed to the fact that the thermal conductivity of the pEG particles is higher than that of P(MA). As the pEG-P(MA) particles are heated, the decomposition of the pEG-P(MA) particles occur both inside and outside of the core–shell particles, making the measured onset temperature be lower than the P(MA). The mass percent of pEG was estimated to be 75.7 wt % in the composite particles by eq. (1) and that of P(MA) was 24.3 wt %.[11]

$$W_{pEG} = \frac{(M_{\mathrm{pEG-P(MA)}} - M_{\mathrm{P(MA)}})}{(M_{\mathrm{pEG}} - M_{\mathrm{P(MA)}})} \times 100\% \quad (1)$$

$$W_{\mathrm{P(MA)}} = 1 - W_{\mathrm{pEG}} \quad (2)$$

where W_{pEG} is the weight percentage of pEG and $W_{\mathrm{P(MA)}}$ is the weight percentage of P(MA) in pEG-P(MA). M_{pEG}, $M_{\mathrm{P(MA)}}$, and $M_{\mathrm{pEG\text{-}P(MA)}}$ are the weight loss of the raw pEG, pure P(MA), and pEG-P(MA), respectively.

Morphological observation of pEG-P(MA)/RPUF composites

The SEM micrographs of pEG/RPUF and pEG-P(MA)/RPUF composites are shown in Figures 4 and 5, respectively. It can be seen from Figure 4(a) that the compatibility between the pEG and RPUF is very poor, resulting in so much collapse and collision of cells, and the relaxedness of the whole cells. From the higher magnification SEM micrograph of the pEG/RPUF composite [Fig. 4(b)], it can be found that the gap between pEG and RPUF is larger than that of the pEG-P(MA) particles and RPUF in Figure 5(b). Therefore, when the matrix is subjected to external force, the stress cannot transfer from the matrix to the pEG particles effectively, causing decline in the mechanical properties.[24] Moreover, the gap is like a chimney, more and continual oxygen would transmit from the outside of material to the internal of material, providing continuous fuel when the composites are burning. Hence, it may make the flame retardancy of the composites degrade.

It can be seen from Figure 5(a) that the cell morphology the pEG-P(MA)/RPUF composites are uniform and integrated. The accumulation of each cell is compacted with each other. No collapses and

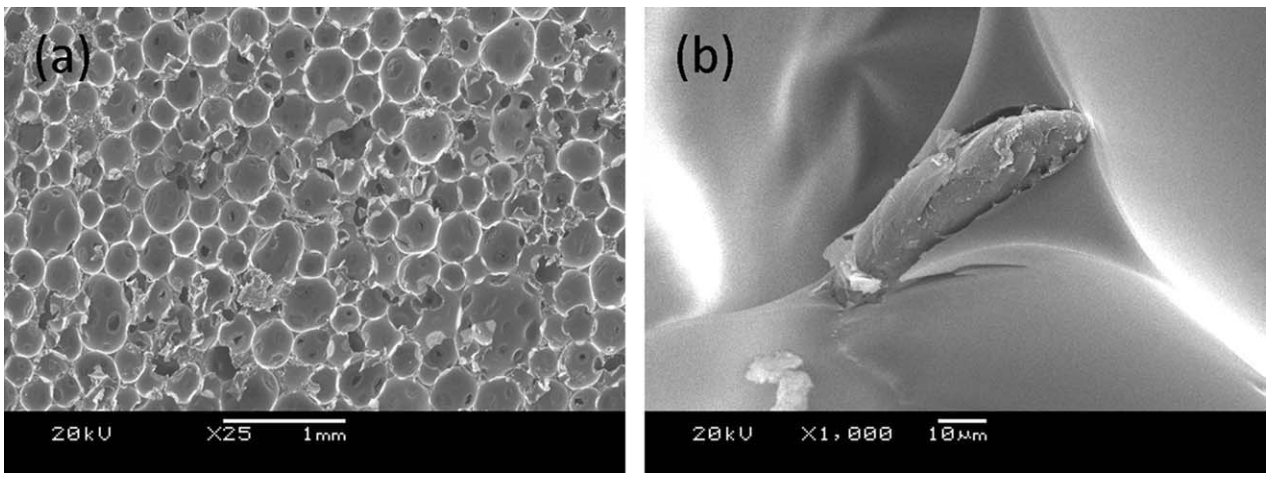

Figure 4 SEM micrographs of the pEG/RPUF at low (a) and high (b) magnification.

collisions exist in the matrix. Figure 5(b) presents the SEM micrographs of the pEG-P(MA)/RPUF composites at higher magnification where the interface between the pEG-P(MA) particles and the RPUF matrix is blurred. Figure 5(c) refers to the enlarged regional areas in Figure 5(b). It can been seen that the pEG-P(MA) particles and the RPUF matrix integrate closely, implying their very good compatibility. The reason for good compatibility is that the core–shell structure can enhance the infiltration of the

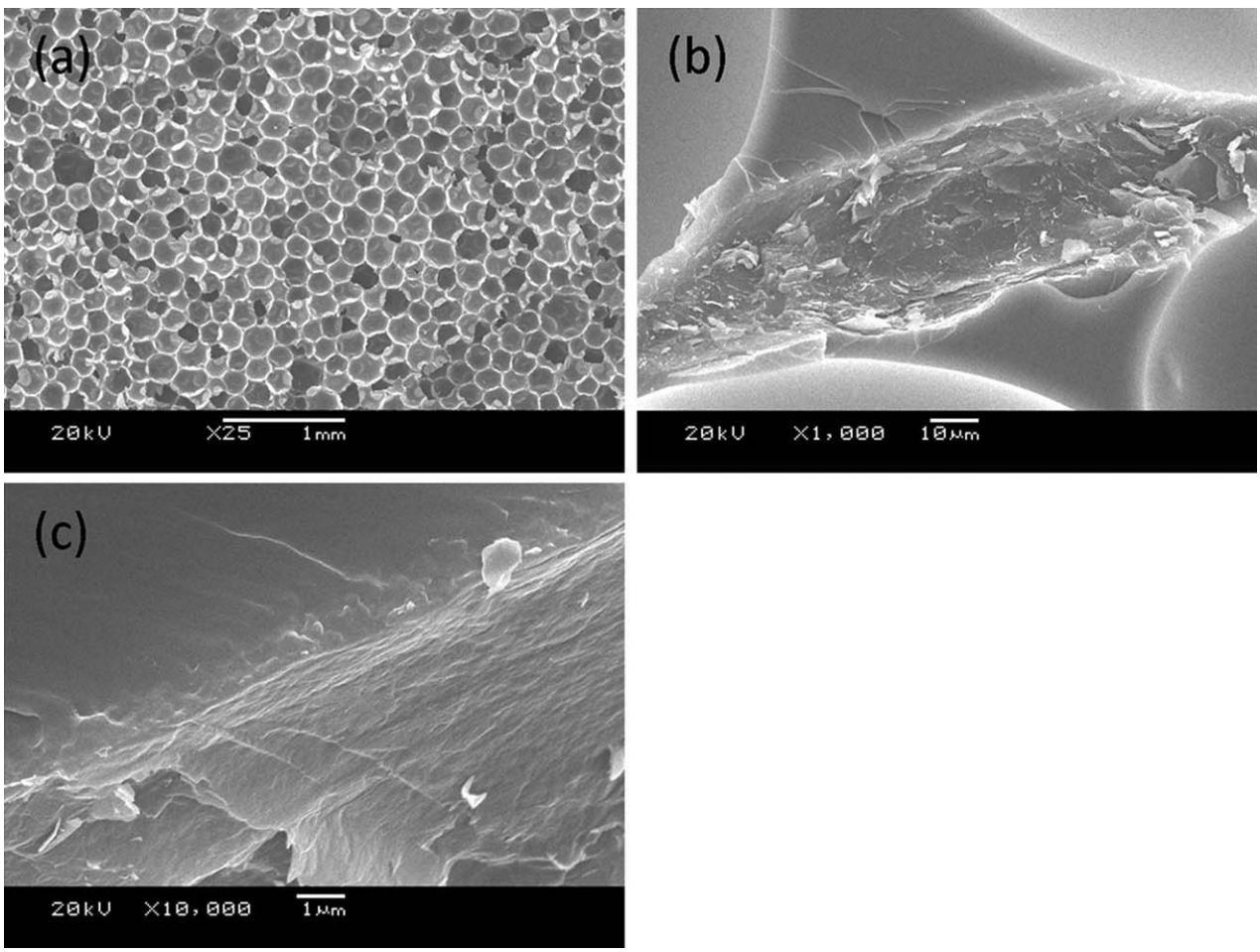

Figure 5 SEM micrographs of the (a) pEG-P(MA)/RPUF at low and high (b, c) magnification.

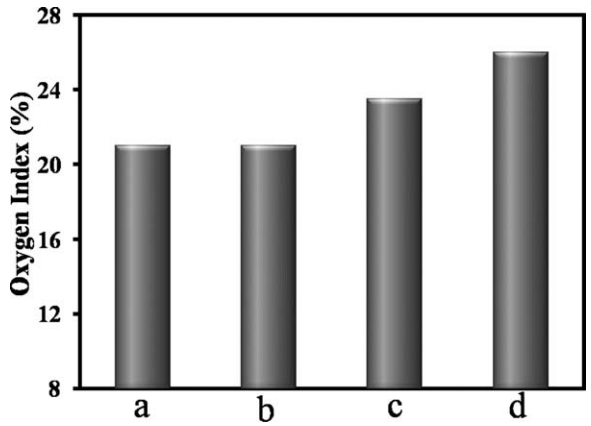

Figure 6 The limiting oxygen index (LOI) values of (a) RPUF, (b) P(MA)/RPUF, (c) pEG/RPUF, and (d) pEG-P(MA)/RPUF.

core–shell particles in the RPUF. At the same time, the —COOH group of copolymer can react with the *R*-NCO group of the isocyanate to produce —COOCOHNR groups as shown in Scheme 2. It is also reported by Zhao[25] that the reaction between toluene 2,4-diisocyanate and carboxylated carbon nanotubes at 50°C can be achieved.

The average diameter of cells is about 330 μm for the pEG/RPUF in Figure 4(a), whereas it is about 250 μm for the pEG-P(MA)/RPUF composite in Figure 5(a). This indicates that the core–shell particles have a good nucleation ability for cell formation, which increases the concentration of cells.[5]

Flame retardant properties of RPUF composites

Figure 6 shows the LOI values of RPUF, P(MA)/RPUF, pEG/RPUF, and pEG-P(MA)/RPUF. As seen from Figure 6, when the pEG is encapsulated by a layer of polymer coating, its LOI gets improved. As the content is 10 wt %, the LOI value increases from 23.5 vol % to 26 vol % compared with that of the pEG/RPUF. The flame retardant properties of pEG-P(MA)/RPUF composite get better than that of the pEG/RPUF composites. It is mainly because when the pEG-P(MA) particles are heated, the polymer coating of P(MA) protects the pEG particles from producing CO_2, H_2O, SO_2 and other gases immediately, hence the graphite sheets fully open and the swelling volume of the pEG particles are bound to be increased.[26] Thus, the flame retardancy can be improved. In addition, with porous structure, thermal conductivity of the thermosetting PUF is extremely poor,[27] therefore the material is likely to cause local accumulation of heat. When the core–shell flame retardant particles are filled into the PUF, the pEG particles may help lead combustion heat away from the burning point, decreasing the thermal insulating efficiency of the foam[28] and the temperature of the fire due to good compatibility between the flame retardant particles and the matrix and good thermal conductivity of graphite, which plays the role of the assisting flame retardant at a certain extent.[29] At the same time, we also find that a small amount of smoke is generated probably due to the decomposition of the P(MA) in the combustion process.

TABLE I
The Horizontal and Vertical Burning Tests for pEG/RPUF, pEG-P(MA) /RPUF, RPUF, and P(MA)/RPUF

Sample	Horizontal burning rate	Vertical burning rate
RPUF	2.33×10^{-3} m/s	–
P(MA)/RPUF	2.58×10^{-3} m/s	–
pEG/RPUF	FH-1	V-1
pEG-P(MA)/RPUF	FH-1	V-1

The data listed in Table I shows the horizontal and vertical burning results of pEG/RPUF, pEG-P(MA)/RPUF, RPUF, and P(MA)/RPUF. With 10 wt % of pEG and pEG-P(MA) content, the composites achieve V-1 rating and FH-1. In addition, we also find that the flame extinguishes immediately after flame application for 30 s. There is no smoke generated in the combustion process. As the content of the P(MA) is 10 wt %, the flame retardant ability of these composites cannot be distinguished merely by the rate of linear burning. Moreover, the rate of linear burning increased to 2.58×10^{-3} m/s from 2.33×10^{-3} m/s with 10 wt % pEG. The reason may be that straight-chain structure of the P(MA) is more lively than the cross-linking structure of polyurethane.

Mechanical properties of RPUF composites

The mechanical properties of RPUF are important parameters to evaluate its practical applications. The compressive strength and modulus of RPUF, pEG/RPUF, pEG-P(MA)/RPUF, and P(MA)/RPUF are shown in Figures 7 and 8. The compressive strength and modulus of RPUF are 2.8 MPa and 48.4 MPa, respectively, while those of the pEG/RPUF are 1.3 MPa and 30.3 MPa. The tremendous decreases are due to poor compatibility between pEG particles and RPUF matrix. However, at the same loading of the pEG-P(MA) particles, there is a marked increase in the compressive strength and modulus, which are 2.29 MPa and 58.46 MPa. Three reasons could clarify the above phenomena, first, the good invasion between pEG-P(MA) and the matrix is conducive to reduce the substrate surface tension. Therefore, the effective contact area between the composite particles and the RPUF matrix increases, enhancing their compatibility which can also be verified in SEM micrographs in Figure 5. Second, reaction between the —COOH and the *R*-NCO establishes

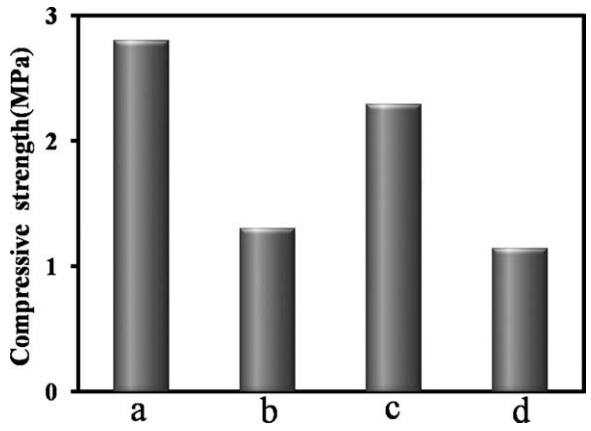

Figure 7 Compressive strength of (a) RPUF, (b) pEG/RPUF, (c) pEG-P(MA)/RPUF, and (d) P(MA)/RPUF.

chemical connections between inorganic particles and RPUF matrix, improving their interface adhesion as formation model in Scheme 2. Moreover, smaller size and higher density of cells would increase the mechanical properties of the foam[30,31] which can be seen from Figures 4 and Figure 5. So when the pEG-P(MA)/RPUF composites suffer from external loading, it can make the stress transfer from matrix to inorganic particles effectively. Moreover, compared with the same loading of pEG-P(MA) particles and P(MA), the compressive strength and modulus of the P(MA)/RPUF are only 1.13 MPa and 26.67 MPa, respectively. Isocyanate could react with PAPI to form cross-linked network structure, which is the key factor to affect mechanical properties. However, cross-linked network structure could be deteriorated to some extent when more —COOH groups of P(MA) react with *R*-NCO groups. Oprea et al.[32] also reported that the different acrylic structural units could depress or improve the mechanical properties of polyurethane materials.

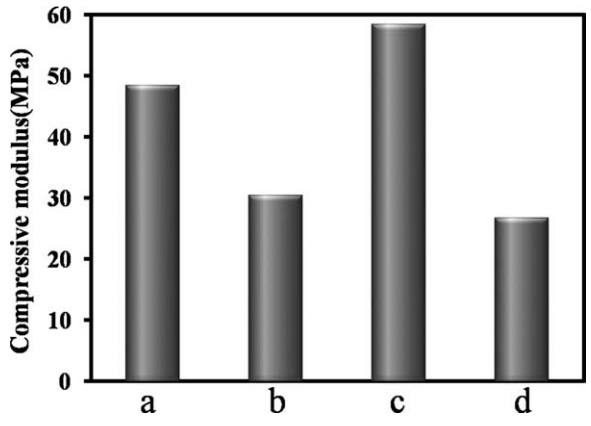

Figure 8 Compressive modulus of (a) RPUF, (b) pEG/RPUF, (c) pEG-P(MA)/RPUF, and (d) P(MA)/RPUF.

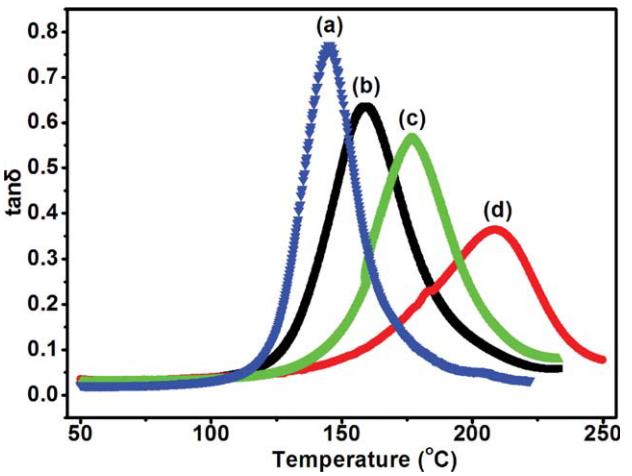

Figure 9 The tan δ of (a) RPUF, (b) pEG-P(MA)/RPUF, (c) P(MA)/RPUF, and (d) pEG/RPUF [Color figure can be viewed in the online issue, which is available at wileyonlinelibrary.com].

This is mainly ascribed to the more —COOH groups of P(MA) which react with the *R*-NCO group, thus reducing the cross-link degree of the matrix and leading to the worse mechanical performance.

In short, good compatibility and effective interface interaction between the inorganic pEG particles and the matrix are very important to improve mechanical properties.[12] When the pEG-P(MA)/RPUF composites are compressed, P(MA) layers exhibit excellent compatibilizing effect and transfer stress effectively. Thereby, damaging pEG-P(MA)/RPUF composite needs more energy, and mechanical properties of the composites have been improved.[33]

Dynamic mechanical analysis of RPUF composites

PUF is often used as package materials, so good damping is necessary for it.[34] The design principle of damping of RPUF composites is to improve the loss factor and glass transition temperature (T_g).[35] Generally, tan δ of damping material should be beyond 0.3.[36] The tan δ of RPUF, pEG/RPUF, pEG-P(MA)/RPUF, and P(MA)/RPUF composites are presented in Figure 9. The tan δ of RPUF (0.77) is higher than that of the pEG/RPUF composite (0.36). Therefore, one can easily conclude that adding pEG particles into the composite depresses the damping properties of the RPUF. The temperature range causing the damping effect of each composite is 130–160°C for RPUF and 195–219°C for pEG/RPUF respectively. However, tan δ of pEG-P(MA)/RPUF composite increases from the 0.36 to 0.63 compared with that of pEG/RPUF composites, while it can be found that the temperature range is 141–180°C. The increase of the temperature range causing damping

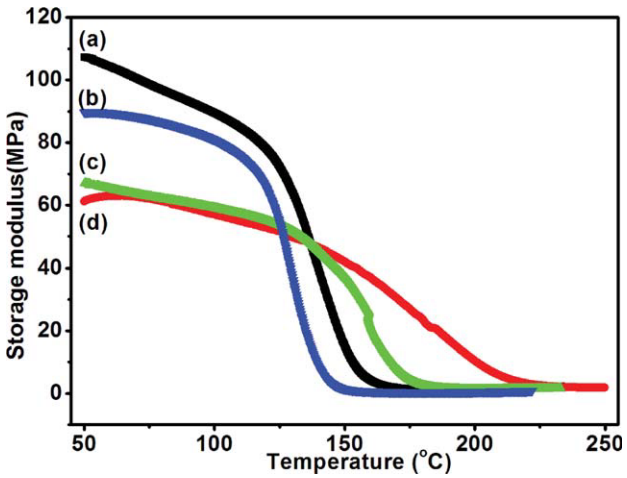

Figure 10 The storage modulus of (a) pEG-P(MA)/RPUF, (b) RPUF, (c) P(MA)/RPUF, and (d) pEG/RPUF [Color figure can be viewed in the online issue, which is available at wileyonlinelibrary.com].

effect should be due to the toughness effect of the P(MA). So the elastic properties of the pEG-P(MA)/RPUF composite become better than that of the pEG/RPUF in relation to tan δ. At the same time, it also can be seen that T_g of the pEG-P(MA)/RPUF composite decreases compared with that of pure RPUF, attributing to the poor cross-link of pEG-P(MA)/RPUF composite. However, tan δ of the P(MA) filled RPUF is only 0.57, while the temperature range is 159–195°C. The damping property of the P(MA)/RPUF composite decreases due to the movement of the smaller segments in P(MA) polymer.

In brief, the damping properties of RPUF are mainly decided by the shape of filler and cross-link degree of the RPUF.[37] Segment movement of the RPUF increases owning to the low degree of cross-linking, then weakening the interlock of network segment.[38–40] At last, the damping performances of the composite are deteriorated. When the cross-linking degree of the composite is too high, it may limit the motion of molecular chains in the network, also undermining the damping properties. Thereby, whether the degree of the cross-linking is too low or too high, the damping properties of the composites would decrease. In short, it is significant to make out the suitable loading of pEG-P(MA) particles that can improve the damping performance of RPUF.

In addition, T_g of the pEG/RPUF and pure RPUF are 207°C and 150°C, respectively, from the TG curves (Fig. 9). The increase of T_g of the pEG/RPUF is attributed to the restriction of molecular motion because of the incorporation of the pEG particles.[41] The rigidness of the P(MA) is lower than that of the pEG particles. Thus increasing movement of molecular chains causes low T_g of the P(MA)/RPUF compared with that of the pure RPUF. The superfluous filler will also reduce the cross-linking degree of the RPUF, leading to lower T_g. So T_g of the pEG-P(MA)/RPUF is lower than that of the P(MA)/RPUF composite.

Figure 10 shows the storage modulus curves of pure RPUF, pEG-P(MA)/RPUF, P(MA)/RPUF, and pEG/RPUF as a function of temperature which are 89.11 MPa, 108.06 MPa, 66 MPa, and 60.65 MPa, respectively, at temperature of 50°C. With the increase of temperature, the storage modulus of all the samples exhibits an obvious falling trend because of the increase of molecular mobility.[42] Particularly at around the glass transition temperature, the storage modulus decreases faster than that at the other temperatures. The storage modulus of pEG-P(MA)/RPUF is the highest before 140°C. The reason may be that the core–shell particles can help improve the storage modulus of the composite due to the better adhesion between the particles and the matrix. Prior to 140°C, the storage modulus of P(MA)/RPUF and pEG/RPUF is always lower than pure RPUF which can be attributed to poor compatibility between the pEG particles and the RPUF matrix. The storage modulus of pEG-P(MA)/RPUF is lower than that of pEG/RPUF when temperature is over 140°C. It is because the macromolecular chains are frozen, while the movement of small segments is accelerated with the increase of the temperature.[43] In short, core–shell particle is helpful to improve the compressive modulus in a certain temperature range.

CONCLUSIONS

SEM and TGA results showed that the core–shell flame retardant particles have been successfully prepared through emulsion polymerization method. The RPUF with the flame retardant particles content of 10 wt % maintained very good flame retardancy (LOI, 26 vol %, V-1 rating in UL-98). It can be seen that a suitable decomposition temperature of the shell material plays a crucial role in flame retardant of the core–shell flame retardant particles. The average diameter of cells indicates that core–shell particles have good nucleation ability for cell formation. The interfacial adhesion between pEG particles and RPUF is propitious to achieve improvement of the mechanical properties of flame retardant RPUF composites. The compressive modulus and the compressive strength of the pEG-P(MA)/RPUF composites were 48.4 MPa and 2.8 MPa, respectively. The DMA test also showed that the core–shell particles could improve the damping performance of pEG-P(MA)/RPUF composites (tan δ 0.77) and the storage modulus (108.06 MPa). Furthermore, the method of encapsulating pEG by the copolymer with respect to the practical application is so simple and quick.

References

1. Duquesne, S.; Michel, L. B.; Bourbigot, S.; Delobel, R.; Poutch, F.; Camino, G.; Eling, B.; Lindsay, C.; Roels T. J Fire Sci 2000, 18, 456.
2. Zaikov, G. E.; Lomakin, S. M. J Appl Polym Sci 2002, 86, 2449.
3. Bourbigot, S.; Michel, L. B.; Decressain, R.; Amoureux, J. P. J Chem Soc Faraday Trans 1996, 92, 149.
4. Modesti, M.; Lorenzetti, A.; Simioni, F.; Camino, G. Polym Degrad Stab 2002, 77, 195.
5. Shi, L.; Li, Z. M.; Yang, M. B.; Yin, B. Polym-Plast Technol Eng 2005, 44, 1323.
6. Shi, L.; Li, Z. M.; Xie, B. H.; Wang, J. H.; Tian, C. R.; Yang, M. B. Polym Int 2006, 55, 862.
7. Bian, X. C.; Tang, J. H.; Li, Z. M.; Lu, Z. Y.; Lu, A. J Appl Polym Sci 2007, 104, 3347.
8. Bian, X. C.; Tang, J. H.; Li, Z. M. J Appl Polym Sci 1935 2008, 109.
9. Bian, X. C.; Tang, J. H.; Li, Z. M. J Appl Polym Sci 2008, 110, 3871.
10. Shi, L.; Li, Z. M.; Wang, J. H.; Yang, M. B.; Zhou, Q. M.; Huang, R. Powder Technol 2006, 170, 178.
11. Ye, L.; Meng, X. Y.; Ji, X.; Li, Z. M.; Tang, J. H. Polym Degrad Stab 2009, 94, 971.
12. Fu, S. Y.; Feng, X. Q.; Lauke, B.; Mai, Y. W. Compos Part B 2008, 39, 933.
13. Camino, G.; Duquesne, S.; Delobel, R.; Eling, B.; Lindsay, C.; Roels, T. 220th ACS National Meeting, 20–24 August 2000, Washington DC: ACS Publishers, 2001, 797, 90.
14. Ni, K. F.; Sheibat-Othman, N.; Shan, G. R.; Fevotte, G.; Bourgeat-Lami, E. Macromolecules 2005, 38, 9100.
15. Mahdavian, A. R.; Ashjari, M.; Makoo, A. B. Eur Polym Mater 2007, 43, 336.
16. Saunders, B. R.; Vincent, B. Adv Colloid Interface Sci 1999, 80, 1.
17. Huang, H. M.; Anker, J. N.; Wang, K. M; Kopelman, R. J Phys Chem B 2006, 110 19929.
18. Leskovac, M.; Kovacevic, V.; Fle, D.; Hace, D. Polym Eng Sci 1999, 39, 600.
19. Jamieson, A.; McNeill, C. Eur Polym Mater 1974, 10, 217.
20. Brown, C. E.; Wilkie, C. A.; Smukalla, J.; Cody, R. B.; Kisinger, J. A. J Polym Sci Polym Chem Ed 1986, 24, 1297.
21. Maurer, J. J.; Eustace, D. J.; Ratcliffe, C. T. Macromolecules 1987, 20, 196.
22. Camino, G.; Sgobbi, R.; Zaopo, A.; Colombier, S.; Scelza, C. Fire Mater 2000, 24, 85.
23. Wang, D. Y.; Cai, X. X.; Qu, M. H.; Liu, Y.; Wang, J. S.; Wang, Y. Z. Polym Degrad Stab 2008, 93, 2186.
24. Saha, M. C.; Kabir, M. E.; Jeelani, S. Mater Sci Eng A 2008, 479, 213.
25. Zhao, C. G.; Ji, L. J.; Liu, H. J.; Hu, G. J.; Zhang, S. M.; Yang, M. S.; Yang, Z. Z. J Solid State Chem 2004, 177, 4394.
26. Modesti, M.; Lorenzetti, A. Polym Degrad Stab 2002, 78, 167.
27. Harikrishnan, G.; Singh, S. N.; Kiesel, E.; Macosko, C.W. Polymer 2010, 51, 3349.
28. Harikrishnan, G.; Patro, U. T.; Khakhar, D. V. Ind Eng Chem Res 2006, 45, 7126.
29. Modesti, M.; Lorenzetti, A. Polym Degrad Stab 2002, 78, 341.
30. Javni, I.; Zhang, W.; Karajkov, V.; Petrovic, Z. S. J Cell Plast 2002, 38, 229.
31. Yin, B.; Li, Z. M.; Quan, H.; Zhou, Q. M.; Tian, C. R.; Yang, M. B. J Elastomers Plast 2004, 36, 333.
32. Oprea, S.; Vlad, S.; Stanciu, A.; Ciobanu, C.; Macoveanu, M. Eur Polym Mater 1999, 35, 1269.
33. Dadbin, S. S.; Chaplin, R. P. J Appl Polym Sci 2001, 81, 3361.
34. Ferreno, D.; Carrascal, I. A.; Cicero, S.; Meng, E. J Test Eval 2010, 38, 211.
35. Petrovic, Z. S.; Javni, I.; Waddon, A.; Bánhegyi G. J Appl Polym Sci 2000, 76, 133.
36. Tung, C. J.; Hsu, T. C. J. J Appl Polym Sci 1992, 46, 1759.
37. Hourston, D. J.; Schäfer, F. U. Polym Adv Technol 1996, 7, 273.
38. Hourston, D. J.; Schäfer, F. U. J. Appl Polym Sci 1996, 2025, 62.
39. Klempner, D.; Frisch, K. C. Lancaster Technomic 1994, IV, 243.
40. Li, Y.; Mao, S. F. J Appl Polym Sci 1996, 61, 2059.
41. Zhong, Z. Y.; Cheng, Y.; Ming, S. Y.; Yiu, W. M. Polym Int 2004, 53, 1093.
42. Narine, S. S.; Kong, X. H.; Bouzidi, L.; Sporns, P. J Am Oil Chem Soc 2007, 84, 65.
43. Manikandan Nair, K. C.; Thomas, S.; Groeninckx, G. Compos Sci Technol 2001, 61, 2519.